PHYSICAL REVIEW D **92,** 023528 (2015)

Ultimate target for dark matter searches

Kfir Blum,[1] Yanou Cui,[2,3] and Marc Kamionkowski[4]

[1]*School of Natural Sciences, Institute for Advanced Study, Princeton, New Jersey 08540, USA*
[2]*Perimeter Institute, 31 Caroline Street North Waterloo, Ontario N2L 2Y5, Canada*
[3]*Maryland Center for Fundamental Physics, Department of Physics, University of Maryland, College Park, Maryland 20742, USA*
[4]*Department of Physics and Astronomy, Johns Hopkins University, 3400 North Charles Street, Baltimore, Maryland 21218, USA*

(Received 16 January 2015; published 22 July 2015)

The combination of S-matrix unitarity and the dynamics of thermal freeze-out for massive relic particles (denoted here simply by WIMPs) implies a *lower* limit on the density of such particles, that provide a (potentially subdominant) contribution to dark matter. This then translates to lower limits to the signal rates for a variety of techniques for direct and indirect detection of dark matter. For illustration, we focus on models where annihilation is s-wave dominated. We derive lower limits to the flux of gamma rays from WIMP annihilation at the Galactic center; direct detection of WIMPs; energetic neutrinos from WIMP annihilation in the Sun; and the effects of WIMPs on the angular power spectrum and frequency spectrum of the cosmic microwave background radiation. The results suggest that a variety of dark-matter-search techniques may provide interesting avenues to seek new physics, even if WIMPs do not constitute all the dark matter. While the limits are quantitatively some distance from the reach of current measurements, they may be interesting for long-range planning exercises.

DOI: 10.1103/PhysRevD.92.023528 PACS numbers: 95.35.+d, 98.35.Gi

Weakly interacting massive particles (WIMPs) provide natural dark matter (DM) candidates and may be experimentally accessible. This has led to much attention in the literature (see, e.g., Refs. [1–3]). DM WIMPs are being sought directly in low-background detectors [4,5], indirectly through searches for gamma rays, cosmic-ray positrons and antiprotons produced by WIMP annihilation in the Galactic halo, and through searches for energetic neutrinos from WIMP annihilation in the Sun and Earth [6,7]. Since these particles arise from new physics beyond the Standard Model, evidence that dark matter is composed of WIMPs would also comprise discovery of new elementary particles. Indeed, such particles are also sought at the Large Hadron Collider (LHC).

There is always the possibility, though, that some new stable massive particle exists but only constitutes a subdominant component of DM [8]. If the particle interacts strongly enough to have been in thermal equilibrium with the Standard Model plasma in the early Universe, then it will still have some nonzero relic density today. Such thermal relics could thus show up in DM searches, even if something else constitutes the majority of the dark matter. Below we refer to stable massive particles with relic abundance dictated by thermal freeze-out broadly as "WIMPs," keeping the name for simplicity even in cases where the particle interacts strongly.

In this paper, we show that the combination of S-matrix unitarity with the dynamics of thermal freeze-out in the early Universe provides *lower* limits to the rates for detection of WIMPs that make up a subdominant, and possibly negligible, contribution to the total DM mass density. Unitarity provides an upper limit to annihilation cross sections, and this has been used to derive an upper limit to the dark matter mass [9] and upper limits to annihilation rates and detection rates for dark matter in the current Universe [10,11]. Still, it is somewhat counterintuitive to think that unitarity can also provide *lower* limits to detection rates. This conclusion, however, follows simply because relic densities are inversely proportional to the WIMP annihilation cross section and so, given the upper limit to that cross section, bounded from below. This then implies lower limits we derive to annihilation rates in the Galactic halo (and thus—given particular final states in the annihilation—to the fluxes of gamma rays, positrons, and antiprotons) and to rates for direct detection and to fluxes of energetic neutrinos from WIMP annihilation in the Sun/Earth. We also derive lower limits to energy deposition from WIMP annihilation in the early Universe, leading to changes to the cosmic microwave background (CMB) angular power spectrum and to the amplitude of CMB spectral distortions. These limits may be valuable in the discussion of long-term goals for the corresponding experimental avenues.

To begin, the relic density of a WIMP χ is $\Omega_\chi h^2 \simeq 0.1(\langle\sigma v\rangle_0/\langle\sigma v\rangle_{\rm fo})$, where Ω_χ is the fraction of the critical density contributed by the WIMP today, $h \simeq 0.7$ the Hubble parameter, $\langle\sigma v\rangle_{\rm fo}$ the thermally averaged velocity-weighted cross section for WIMP annihilation (to all channels), calculated at the time of freeze-out, and the constant $\langle\sigma v\rangle_0 \simeq 3\times 10^{-26}\ {\rm cm}^3\ {\rm sec}^{-1}$ arises from the

dynamics of thermal freeze-out. For a pair of nonrelativistic WIMPs annihilating with relative velocity v, partial-wave unitarity dictates an upper bound [9] $\sigma_L \leq 4\pi(2L+1)/(m_\chi^2 v^2)$, where m_χ is the WIMP mass and σ_L is the partial cross section for reaction with orbital angular momentum L. In what follows we focus on the case where WIMP annihilation is s-wave, or $L = 0$. We then have

$$\langle\sigma v\rangle_{\rm fo} \leq 4\pi\langle v^{-1}\rangle_{\rm fo}/m_\chi^2, \tag{1}$$

where $\langle v^{-1}\rangle_{\rm fo} = \sqrt{m_\chi/(\pi T_{\rm fo})} \simeq 2.5$ is the thermally averaged inverse relative velocity, using the typical value $m_\chi/T_{\rm fo} = 20$. There then follows a lower limit,

$$\Omega_\chi/\Omega_{\rm dm} \geq (m_\chi/110\ {\rm TeV})^2, \tag{2}$$

to the relic density of WIMPs, in units of the observed DM density $\Omega_{\rm dm}$, and where the numerical value is updated from Ref. [9] using the current value $\Omega_{\rm dm}h^2 \simeq 0.11$ [12,13]. The usual unitarity limit $m_\chi \leq 110$ TeV to the WIMP mass follows from the requirement $\Omega_\chi \leq \Omega_{\rm dm}$. Improved analysis on the prediction of a thermal relic DM abundance [14] may give up to O(1) change in Eq. (2), which is nonetheless a sufficiently good approximation for the precision goal of this study.

We now consider gamma rays from DM annihilation in the halo of the Milky Way. The search for such gamma rays is actively under way; it is one of the principal science goals of the Fermi Telescope [15,16] and will also be a target for the Cherenkov Telescope Array (CTA) [17]. The annihilation rate density is

$$Q_\chi = \rho_\chi^2\langle\sigma v\rangle_h/(4m_\chi^2), \tag{3}$$

where ρ_χ is the WIMP mass density and $\langle\sigma v\rangle_h$ is the velocity averaged annihilation cross section times relative velocity in the Galactic halo. (If χ is self-conjugate, then the factor of $1/4$ on the right-hand side above should be replaced by $1/2$.) If χ constitutes a fraction $\Omega_\chi/\Omega_{\rm dm}$ of the DM, then its density in the Galactic halo will be $(\Omega_\chi/\Omega_{\rm dm})\rho_h$, where ρ_h is the Galactic-halo density. For the s-wave annihilations we consider here, neglecting effects such as Sommerfeld enhancement or suppression, $\langle\sigma v\rangle_{\rm fo} = \langle\sigma v\rangle_h$. Then, using $\Omega_\chi/\Omega_{\rm dm} \approx \langle\sigma v\rangle_0/\langle\sigma v\rangle_{\rm fo}$ and Eq. (1), we find a lower limit,

$$Q_\chi \geq \frac{\rho_h^2(\langle\sigma v\rangle_0)^2}{16\pi\langle v^{-1}\rangle_{\rm fo}}, \tag{4}$$

independent of m_χ and $\langle\sigma v\rangle_{\rm fo}$ up to logarithmic corrections.

The differential gamma-ray flux from a window of solid angle $\Delta\Omega$ around a given line of sight is

$$J_\gamma(E_\gamma) = \int_{\Delta\Omega}\frac{d\Omega}{4\pi}\int dr Q_\chi(r)\frac{dN}{dE_\gamma}, \tag{5}$$

where the integral is along the line of sight, $Q_\chi(r)$ is evaluated at a distance r along that line of sight, and dN/dE_γ is the differential number of photons of energy E_γ per annihilation event. Using Eq. (4), we have

$$\begin{aligned} J_\gamma(E_\gamma) &\geq \frac{\bar{J}(\langle\sigma v\rangle_0)^2}{64\pi^2\langle v^{-1}\rangle_{\rm fo}}\frac{dN}{dE_\gamma} \\ &\simeq 10^{-16}\left(\frac{dN}{dE_\gamma}\right)\left(\frac{\bar{J}}{\bar{J}_{\rm nfw,gc}}\right)\ {\rm cm}^{-2}\,{\rm sec}^{-1}, \end{aligned} \tag{6}$$

where $\bar{J} = \int_{\Delta\Omega} d\Omega \int dr \rho_h^2$ is the line-of-sight integral. We have evaluated this quantity in the second line in terms of the value $\bar{J}_{\rm nfw,gc} \simeq 2.5 \times 10^{21}\ {\rm GeV}^2\,{\rm cm}^{-5}$ obtained for the HESS Galactic-center region of interest [18] (a circle of radius 1° around the Galactic center with a Galactic-plane mask to remove $|b| < 0.3^\circ$) using the NFW profile [19] $\rho_h(r) = \rho_0(r_s/r)(1+r/r_s)^{-2}$, with $\rho_0 = 0.4$ GeV cm^{-3} and $r_s = 20$ kpc. Besides the Galactic center, another target of interest in gamma-ray searches for DM are Milky Way dwarf galaxies, where $\bar{J}/\bar{J}_{\rm nfw,gc} \sim 10^{-4} - 10^{-3}$ (see, e.g., Ref. [20]) but astrophysical backgrounds are smaller.

We can assess the implications of the lower limit to the gamma-ray flux of a thermal relic by projecting it onto the sensitivity plot for gamma-ray experiments. These experiments typically show curves of $\langle\sigma v\rangle$ versus m_χ, where the $\langle\sigma v\rangle$ plotted is the value inferred from a given gamma-ray flux, assuming that the WIMP comprises *all* the DM. In other words, $\langle\sigma v\rangle$ is a proxy for (and proportional to) the gamma-ray flux J_γ; i.e., $\langle\sigma v\rangle \propto J_\gamma m_\chi^2/\bar{J}$ [cf. Eq. (3)].

Figure 1 shows such a plot. Shown as a gray horizontal band is the value $\langle\sigma v\rangle_0$ that arises if the WIMP makes up all the DM. The black line indicates the upper limit on $\langle\sigma v\rangle$ directly imposed by unitarity [cf. Eq. (1)]. The cyan and purple curves show an estimate [21] of the smallest flux detectable with 500 hours of observation with CTA, under two different assumptions about annihilation products. The red line indicates the smallest flux possible for a subdominant thermal relic. Clearly, there is plenty of parameter space that gives rise to gamma-ray flux well below those that will be accessible with CTA. However, if there is any stable thermal relic WIMP from the big bang, and assuming that the annihilation is s-wave dominated with final states consisting of charged Standard Model fermions or massive gauge bosons, as in Fig. 1 (and as is usually done in the corresponding gamma-ray analyses), subsequent generations of detectors that improve the sensitivity sufficiently to reach our unitarity limit should be sensitive to the annihilation gamma-ray signal even if that relic does not account for the majority of the DM. For example, a telescope with a sensitivity improvement over CTA of 3

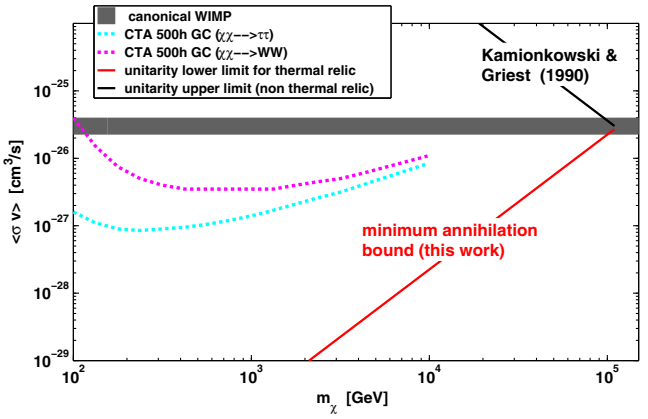

FIG. 1 (color online). Thermal averaged cross section times relative velocity $\langle\sigma v\rangle$ versus WIMP mass m_χ. The horizontal gray band shows the canonical cross section for a thermal relic making up the dark matter. The black line is the largest annihilation cross section consistent with unitarity. The purple and cyan curves show an estimate of the smallest $\langle\sigma v\rangle$ detectable by CTA with 500 hours of observation time [21], assuming annihilation to $\tau^+\tau^-$ or W^+W^- pairs, and assuming that the WIMP makes up all the halo dark matter. The red line shows the smallest inferred $\langle\sigma v\rangle$ that would be possible for a subdominant WIMP.

orders of magnitude will see a signal from any thermal relic heavier than about a TeV.

We now move on to direct detection of WIMPs. The precise expression for the rate for direct detection of WIMPs depends on a variety of factors, including the DM velocity distribution in the Galactic halo and energy dependence of the WIMP-nucleus elastic-scattering cross section. If we approximate the halo DM velocity distribution as a Maxwell-Boltzmann distribution, the event rate per unit mass in a DM detector is [1] $\Gamma = (2/\sqrt{\pi})\rho_\chi v_0 \sigma_N/(m_\chi m_N)$, where $v_0 \simeq 220$ km sec^{-1} is the halo circular speed, σ_N is the cross section for elastic scattering of the WIMP from the nucleus, and m_N the target-nucleus mass. The cross section for WIMP scattering off a nucleus of mass number A is related to the WIMP-nucleon cross section $\sigma_{\chi p(n)}$. For instance, assuming spin-independent (SI) interaction without isospin violation, the relation is $\sigma_N = (A^2\mu_{\chi p}^2/\mu_{\chi N}^2)\sigma_{\chi p}$, where $\mu_{\chi p}$ and $\mu_{\chi N}$ are the reduced masses of the χ-proton and χ-nucleus systems respectively. Replacing ρ_χ by the unitarity limit $\rho_h(\Omega_\chi/\Omega_{\rm dm}) \geq \rho_h(m_\chi/110\ {\rm TeV})^2$, we infer that the rate for detection of a WIMP with elastic cross section σ_N must satisfy

$$\Gamma \geq \frac{2}{\sqrt{\pi}}\frac{\rho_h v_0 \sigma_N}{m_\chi m_N}\left(\frac{m_\chi}{110\ {\rm TeV}}\right)^2. \quad (7)$$

Again, the sensitivity of direct DM searches are usually shown as plots of the WIMP-proton scattering cross section $\sigma_{\chi p}$ versus WIMP mass m_χ (with an additional constraint for $\sigma_{\chi n}$ for spin-dependent (SD) interaction). These constraint plots then show the largest such cross section allowed based

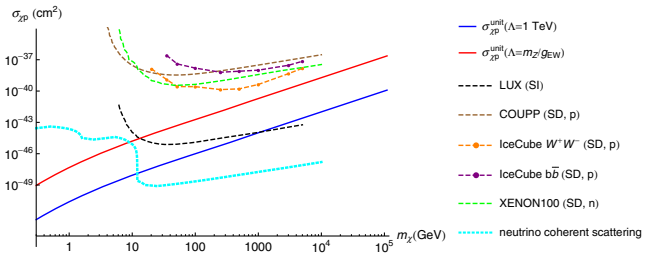

FIG. 2 (color online). WIMP-proton elastic-scattering cross section versus WIMP mass m_χ. Dashed lines show the current upper limits by various experiments, assuming that χ makes up all the dark matter. Solid blue and red lines denote the minimal effective WIMP-nucleon cross sections inferred from the unitarity limit, for two different values of the actual scattering cross section $\sigma_{\chi p}^{\rm actual} = \mu_{\chi p}^2/\pi\Lambda^4$, corresponding to $\Lambda = 1$ TeV and $\Lambda \simeq m_Z/g_{\rm EW}$, respectively. The dotted cyan band shows the effective cross section at which coherent scattering from background neutrinos becomes significant [22].

on a given experiment, assuming that the WIMP makes up all the DM. In Fig. 2 we show the smallest nominal cross section $\sigma_{\chi p}^{\rm unit}$ for a subdominant WIMP, obtained from our unitarity argument, which would be inferred in this way, for different values of *actual* scattering cross section $\sigma_{\chi p}^{\rm actual}$. According to Eq. (7), we have the relation $\sigma_{\chi p}^{\rm unit} \simeq (m_\chi/110\ {\rm TeV})^2\sigma_{\chi p}^{\rm actual}$. The actual scattering cross section $\sigma_{\chi p}^{\rm actual}$, both SI and SD, in general can be parametrized by an effective mass scale Λ with $\sigma_{\chi p}^{\rm actual} = \mu_{\chi p}^2/(\pi\Lambda^4)$. Note that at large WIMP mass $m_\chi \gg m_p$, $\sigma_{\chi p}^{\rm actual}$ is independent of m_χ for a fixed Λ.

It is impossible to correlate in a model-independent way the actual DM-nucleon scattering cross section $\sigma_{\chi p}^{\rm actual}$ and the total thermal annihilation cross section constrained by unitarity. In Fig. 2, for illustration, we therefore chose two arbitrary examples, one with $\Lambda = 1$ TeV and one with the Standard Model Z boson as the mediator for DM-nucleon scattering, i.e., $\Lambda \simeq m_Z/g_{\rm EW}$. In addition to the unitarity lower bounds as applied to our two examples for Λ, we also show the current upper bounds on SI scattering from LUX, as well as limits on SD scattering from IceCube, XENON100 and COUPP [23–26]. To emphasize why Fig. 2 is interesting, note that, for example, we learn from it that a massive ($m_\chi \gtrsim 10$ GeV) thermal relic Dirac fermion or charged scalar WIMP, with s-wave dominated annihilation and elastic scattering, cannot be charged under the Standard Model $SU(2)_W$ gauge group. As far as we know, this is a novel observation: before this paper, a simple naive way out for such a model could have been to simply assign the WIMP with some very efficient mode of annihilation, such that its relic abundance would be small enough to avoid detection despite an $SU(2)_W$ charge. Unitarity excludes this possibility.

Limits from IceCube are directly based on energetic neutrinos from WIMPs that are captured and then

annihilate in the Sun. They therefore depend on annihilation final states and assume that the capture and annihilation equilibrate, in which case the annihilation rate is equal to half of the capture rate. This equilibration occurs, though, only if the equilibration time scale [27],

$$\tau = 1.6\times 10^5\ \mathrm{yr}[\rho_{\chi,0.4}\langle\sigma v\rangle_{26} f(m_\chi)]^{-1/2} \times (m_\chi/100\ \mathrm{GeV})^{-3/4}\sigma_{40}^{-1/2}, \quad (8)$$

is shorter than the age, $\sim 5\times 10^9$ yr, of the Sun. Here, $\rho_{\chi,0.4}$ is the WIMP density in units of 0.4 GeV cm^{-3}, $f(m_\chi)\sim O(1)$ is given in Ref. [28], $\langle\sigma v\rangle_{26}$ the annihilation cross section times relative velocity in units of 10^{-26} cm^3 sec^{-1}, and $\sigma_{40}=\sigma_{\chi p}/(10^{-40}\ \mathrm{cm}^2)$. As Eq. (8) indicates, the equilibration time scale increases if the halo WIMP density ρ_χ decreases, or if the annihilation cross section $\langle\sigma v\rangle_{26}$ decreases. However, for a thermal relic WIMP, the combination $\rho_{\chi,0.4}\langle\sigma v\rangle_{26}$ that appears in Eq. (8) remains constant as the annihilation cross section (and thus relic density) is changed. As a consequence, the energetic-neutrino flux for these subdominant WIMPs is indeed controlled by the elastic-scattering cross section, as long as $\sigma_{\chi p}\gtrsim (m_\chi/100\ \mathrm{GeV})^{-3/2}10^{-49}$ cm^2.

We now turn to the effects of subdominant WIMP annihilation on CMB fluctuations and spectral distortions. WIMP annihilation continuously injects a small amount of energy into the cosmic plasma throughout the history of the Universe. Annihilations in the redshift range of roughly $z\sim 10^3-10^6$ heat the plasma during a time when photons cannot fully reequilibrate thermally, giving rise to distortions in the CMB frequency spectrum [29]. Annihilations that occur around the time of recombination alter slightly the ionization history of the Universe and thus the detailed angular power spectrum of CMB temperature and polarization fluctuations [30].

The quantity of interest for CMB analysis is the rate density $\dot{u}=\rho_\chi^2\langle\sigma v\rangle/(2m_\chi)$, for energy injection due to WIMP annihilation, where here ρ_χ is the cosmic density of WIMP χ at any particular redshift. Current measurements of angular CMB power spectra imply an upper limit [12,13],

$$\left(\frac{\rho_\chi}{\rho_{\mathrm{dm}}}\right)^2\left(\frac{f\langle\sigma v\rangle}{\langle\sigma v\rangle_0}\right)\left(\frac{m_\chi}{10\ \mathrm{GeV}}\right)^{-1}\lesssim 1, \quad (9)$$

or equivalently,

$$\dot{u}f\lesssim \dot{u}_{\mathrm{ion,max}}=\rho_{\mathrm{dm}}^2\langle\sigma v\rangle_0/(20\ \mathrm{GeV}). \quad (10)$$

Here, the quantity $f\sim 0.1-1$ parametrizes the fraction of the injected energy that gets absorbed by the plasma [31,32]. The precise value of f depends on the particular WIMP annihilation channels and also to some extent on m_χ. Assuming $\langle\sigma v\rangle\simeq\langle\sigma v\rangle_{\mathrm{fo}}$, unitarity implies a lower limit,

$$\dot{u}\geq m_\chi\rho_{\mathrm{dm}}^2(\langle\sigma v\rangle_0)^2/(8\pi\langle v^{-1}\rangle_{\mathrm{fo}}), \quad (11)$$

where $\rho_{\mathrm{dm}}(z)=\Omega_{\mathrm{dm}}\rho_c(1+z)^3$ is the cosmic DM density at redshift z. Using Eq. (11), we have

$$\frac{\dot{u}f}{\dot{u}_{\mathrm{ion,max}}}\geq\frac{5f\langle\sigma v\rangle_0 m_\chi\ \mathrm{GeV}}{2\pi\langle v^{-1}\rangle_{\mathrm{fo}}} \simeq 2\times 10^{-5}\left(\frac{f}{0.3}\right)\left(\frac{m_\chi}{100\ \mathrm{TeV}}\right). \quad (12)$$

To give a more physical representation of the effect of WIMP annihilation, consider the contribution $\Delta\tau$ to the Thomson optical depth for CMB photons, caused due to the excess free electrons resulting from the annihilation. We can give an analytical estimate of $\Delta\tau$ by integrating the excess Thomson scattering over redshift, starting from the redshift $\bar{z}\approx 1100$ at which recombination freezes out. This yields

$$\begin{aligned}\Delta\tau_{\bar{z}} &\approx \int_0^{\bar{z}}\frac{dzc\sigma_T n_H(z)}{H(z)(1+z)}\int_z^{\bar{z}}\frac{dz'\dot{u}(z')f}{3\epsilon_H n_H(z')H(z')(1+z')}\\ &\approx \frac{c\sigma_T\langle\sigma v\rangle_0\Omega_{\mathrm{dm}}^2H_0^2\bar{z}^3}{96\pi^2G_N^2\epsilon_H(20\ \mathrm{GeV})}\frac{\dot{u}f}{\dot{u}_{\mathrm{ion,max}}}\\ &\approx 0.07\left(\frac{\bar{z}}{1100}\right)^3\left(\frac{f\dot{u}}{\dot{u}_{\mathrm{ion,max}}}\right).\end{aligned} \quad (13)$$

Here ϵ_H is the ionization energy of hydrogen, σ_T is the Thomson cross section, and G_N is the gravitational constant. The analytical result above is useful for clarifying the parameter dependence of the process, but it slightly overestimates the actual effect, because of some residual recombination of the excess free electrons. Modifying the standard recombination code RECFAST [33] to account for the effect, we find numerically $\Delta\tau_{1100}\approx 0.05(f\dot{u}/\dot{u}_{\mathrm{ion,max}})$, valid for $\dot{u}\lesssim\dot{u}_{\mathrm{ion,max}}$, where we have defined $\Delta\tau_{1100}$ to be the integrated optical depth from today up to redshift $z=1100$ (note that the linear relation between $\Delta\tau$ and $\dot{u}$ breaks down for $\dot{u}\gtrsim\dot{u}_{\mathrm{ion,max}}$ [34]). Using the numerical result, then, we find that unitarity gives $\Delta\tau_{1100}\gtrsim 10^{-6}(\frac{f}{0.3})(\frac{m_\chi}{100\ \mathrm{TeV}})$ or so. For comparison, current constraints [13] on the low-redshift optical depth due to reionization imply $\tau=0.089\pm 0.013$.

Energy injection at redshifts $5\times 10^4\lesssim z\lesssim 2\times 10^6$ (the μ era) give rise to μ distortions to the CMB frequency spectrum, and injection at redshifts $10^3\lesssim z\lesssim 5\times 10^4$ (the y era), give rise primarily to Compton-y distortions. The current limits from the COBE/FIRAS [35] experiment are $|\mu|\lesssim 10^{-4}$ and $|y|\lesssim 10^{-5}$. Future measurements by PIXIE [36] should reach a sensitivity of $\mu, y\sim 10^{-8}$ at 5σ, and PRISM [37] could get to values several orders of magnitude smaller. Energy injection during the μ era that changes the thermal energy density in the plasma by a fractional amount $(\Delta\rho_\gamma/\rho_\gamma)$ gives rise to a μ distortion of magnitude $\mu\simeq 1.4(\Delta\rho_\gamma/\rho_\gamma)$, while that during the y era gives rise to $y\simeq 0.25(\Delta\rho_\gamma/\rho_\gamma)$ [29]. Annihilation during the μ era thus lead to [29]

$$\mu \simeq 4\times 10^{-8}(1-f_\nu)\left(\frac{\rho_\chi}{\rho_{\rm dm}}\right)^2\left(\frac{\langle\sigma v\rangle}{\langle\sigma v\rangle_0}\right)\left(\frac{10\,{\rm GeV}}{m_\chi}\right), \quad (14)$$

where f_ν is the fraction of the annihilation energy carried away by neutrinos, ranging between zero to tens of percent for typical annihilation final states. We can then write a lower bound,

$$\mu \gtrsim 3\times 10^{-12}(1-f_\nu)(m_\chi/100\ {\rm TeV}), \quad (15)$$

based on unitarity, to the μ distortion. For comparison, the not precisely adiabatic cooling of primordial gas, as well as the dissipation of small-scale acoustic waves, give rise to μ distortions at the level of $\mu \sim 10^{-8}$ [29]. We note, though, that detailed spectrum measurements may help to disentangle a DM annihilation signal from other cosmic sources of spectral distortions [38].

To recapitulate, rates for direct and indirect detection of subdominant WIMPs all depend either linearly or quadratically on their relic density. A lower limit to the density of a thermal relic is set by the upper limit imposed by unitarity to its annihilation cross section. Thus, under common assumptions for the annihilation final states or for the WIMP-nucleon elastic scattering cross section, the signals expected from subdominant WIMPs cannot be arbitrarily small. Here we have discussed direct WIMP detection at low-background dark matter detectors, gamma rays from WIMP annihilation at the Galactic center, energetic neutrinos from WIMP annihilation in the Sun, and the effects of WIMPs on the angular power spectra and frequency spectrum of the CMB. There are likewise lower limits to the flux of cosmic-ray positrons and antiprotons and to the effects of WIMP annihilation on 21-cm fluctuations from the dark ages [39,40].

There are, of course, some caveats. First of all, we have focused on WIMPs with s-wave annihilation. Quantitative results may differ for p-wave annihilation or for WIMPs with Sommerfeld enhancements, but in either case there will be limits that remain. The limits do not necessarily apply for WIMPs that have nonthermal cosmic densities, primordial particle-antiparticle asymmetry, efficient coannihilation, or if there was a significant amount of post-freeze-out entropy production. If the main annihilation channel of the WIMP is into stable dark-sector states such as dark radiation [41,42], the limits for indirect searches and CMB signals we derived here will bear a branching-fraction suppression. There are also caveats, though, that may strengthen the bounds. For example, the unitarity argument we have used is conservative and may be made more restrictive for large classes of WIMP models [43]. To close, though, it is of interest that simple considerations lead to a fairly general lower limit to the rates for detection of thermal relics, even if they do not make up most of the dark matter.

M. K. thanks J. Chluba for useful discussions. K. B. was supported by DOE Grant No. DE-SC000998, the BSF, and the Bahcall Fellow Membership. Y. C. is supported by Perimeter Institute for Theoretical Physics, which is supported by the Government of Canada through Industry Canada and by the Province of Ontario through the Ministry of Research and Innovation. Y. C. is in part supported by NSF Grant No. PHY-0968854 and by the Maryland Center for Fundamental Physics. M. K. was supported by the John Templeton Foundation, the Simons Foundation, NSF Grant No. PHY-1214000, and NASA ATP Grant No. NNX15AB18G.

[1] G. Jungman, M. Kamionkowski, and K. Griest, Supersymmetric dark matter, Phys. Rep. **267**, 195 (1996).
[2] L. Bergstrom, Nonbaryonic dark matter: Observational evidence and detection methods, Rep. Prog. Phys. **63**, 793 (2000).
[3] G. Bertone, D. Hooper, and J. Silk, Particle dark matter: Evidence, candidates and constraints, Phys. Rep. **405**, 279 (2005).
[4] M. W. Goodman and E. Witten, Detectability of certain dark matter candidates, Phys. Rev. D **31**, 3059 (1985).
[5] I. Wasserman, Possibility of detecting heavy neutral fermions in the galaxy, Phys. Rev. D **33**, 2071 (1986).
[6] J. Silk, K. A. Olive, and M. Srednicki, The Photino, the Sun and High-Energy Neutrinos, Phys. Rev. Lett. **55**, 257 (1985).
[7] M. Kamionkowski, Energetic neutrinos from heavy neutralino annihilation in the sun, Phys. Rev. D **44**, 3021 (1991).
[8] G. Duda, G. Gelmini, P. Gondolo, J. Edsjo, and J. Silk, Indirect detection of a subdominant density component of cold dark matter, Phys. Rev. D **67**, 023505 (2003).
[9] K. Griest and M. Kamionkowski, Unitarity Limits on the Mass and Radius of Dark Matter Particles, Phys. Rev. Lett. **64**, 615 (1990).
[10] J. F. Beacom, N. F. Bell, and G. D. Mack, General Upper Bound on the Dark Matter Total Annihilation Cross Section, Phys. Rev. Lett. **99**, 231301 (2007).
[11] L. Hui, Unitarity Bounds and the Cuspy Halo Problem, Phys. Rev. Lett. **86**, 3467 (2001).
[12] G. Hinshaw *et al.* (WMAP Collaboration), Nine-year Wilkinson Microwave Anisotropy Probe (WMAP)

observations: Cosmological parameter results, Astrophys. J. Suppl. Ser. **208**, 19 (2013).
[13] P. A. R. Ade *et al.* (Planck Collaboration), Planck 2013 results. XVI. Cosmological parameters, Astron. Astrophys. **571**, A16 (2014).
[14] P. Gondolo and G. Gelmini, Cosmic abundances of stable particles: Improved analysis, Nucl. Phys. **B360**, 145 (1991).
[15] M. Ackermann *et al.* (Fermi-LAT Collaboration), Constraining Dark Matter Models from a Combined Analysis of Milky Way Satellites with the Fermi Large Area Telescope, Phys. Rev. Lett. **107**, 241302 (2011).
[16] M. Ackermann *et al.* (Fermi-LAT Collaboration), Fermi-LAT observations of the diffuse gamma-ray emission: Implications for cosmic rays and the interstellar medium, Astrophys. J. **750**, 3 (2012).
[17] S. Vercellone (Consortium for the CTA Collaboration), The next generation Cherenkov Telescope Array observatory: CTA, arXiv:1405.5696.
[18] A. Abramowski *et al.* (HESS Collaboration), Search for a Dark Matter Annihilation Signal from the Galactic Center Halo with H.E.S.S, Phys. Rev. Lett. **106**, 161301 (2011).
[19] J. F. Navarro, C. S. Frenk, and S. D. M. White, Structure of cold dark matter halos, Astrophys. J. **462**, 563 (1996).
[20] A. Abramowski *et al.* (HESS Collaboration), H.E.S.S. constraints on dark matter annihilations towards the Sculptor and Carina dwarf galaxies, Astropart. Phys. **34**, 608 (2011).
[21] M. Wood, J. Buckley, S. Digel, S. Funk, D. Nieto, and M. A. Sanchez-Conde, Prospects for indirect detection of dark matter with CTA, arXiv:1305.0302.
[22] J. Billard, L. Strigari, and E. Figueroa-Feliciano, Implication of neutrino backgrounds on the reach of next generation dark matter direct detection experiments, Phys. Rev. D **89**, 023524 (2014).
[23] E. Aprile *et al.* (XENON100 Collaboration), Limits on Spin-Dependent WIMP-Nucleon Cross Sections from 225 Live Days of XENON100 Data, Phys. Rev. Lett. **111**, 021301 (2013).
[24] E. Behnke *et al.* (COUPP Collaboration), First dark matter search results from a 4-kg CF_3I bubble chamber operated in a deep underground site, Phys. Rev. D **86**, 052001 (2012); **90**, 079902(E) (2014).
[25] M. G. Aartsen *et al.* (IceCube Collaboration), Search for Dark Matter Annihilations in the Sun with the 79-string IceCube Detector, Phys. Rev. Lett. **110**, 131302 (2013).
[26] D. S. Akerib *et al.* (LUX Collaboration), First Results from the LUX Dark Matter Experiment at the Sanford Underground Research Facility, Phys. Rev. Lett. **112**, 091303 (2014).
[27] S. M. Koushiappas and M. Kamionkowski, Galactic Substructure and Energetic Neutrinos from the Sun and the Earth, Phys. Rev. Lett. **103**, 121301 (2009).
[28] M. Kamionkowski, K. Griest, G. Jungman, and B. Sadoulet, Model Independent Comparison of Direct Versus Indirect Detection of Supersymmetric Dark Matter, Phys. Rev. Lett. **74**, 5174 (1995).
[29] J. Chluba and R. A. Sunyaev, The evolution of CMB spectral distortions in the early Universe, Mon. Not. R. Astron. Soc. **419**, 1294 (2012).
[30] N. Padmanabhan and D. P. Finkbeiner, Detecting dark matter annihilation with CMB polarization: Signatures and experimental prospects, Phys. Rev. D **72**, 023508 (2005).
[31] X. L. Chen and M. Kamionkowski, Particle decays during the cosmic dark ages, Phys. Rev. D **70**, 043502 (2004).
[32] T. R. Slatyer, Energy injection and absorption in the cosmic dark ages, Phys. Rev. D **87**, 123513 (2013).
[33] S. Seager, D. D. Sasselov, and D. Scott, How exactly did the universe become neutral?, Astrophys. J. Suppl. Ser. **128**, 407 (2000).
[34] C. Dvorkin, K. Blum, and M. Zaldarriaga, Perturbed recombination from dark matter annihilation, Phys. Rev. D **87**, 103522 (2013).
[35] D. J. Fixsen, E. S. Cheng, J. M. Gales, J. C. Mather, R. A. Shafer, and E. L. Wright, The cosmic microwave background spectrum from the full COBE FIRAS data set, Astrophys. J. **473**, 576 (1996).
[36] A. Kogut, D. J. Fixsen, D. T. Chuss, J. Dotson, E. Dwek, M. Halpern, G. F. Hinshaw, S. M. Meyer *et al.*, Primordial inflation explorer (PIXIE): A nulling polarimeter for cosmic microwave background observations, J. Cosmol. Astropart. Phys. 07 (2011) 025.
[37] P. Andre *et al.* (PRISM Collaboration), PRISM (polarized radiation imaging and spectroscopy mission): A white paper on the ultimate polarimetric spectro-imaging of the microwave and far-infrared sky, arXiv:1306.2259.
[38] J. Chluba and D. Jeong, Teasing bits of information out of the CMB energy spectrum, Mon. Not. R. Astron. Soc. **438**, 2065 (2014).
[39] S. R. Furlanetto, S. P. Oh, and E. Pierpaoli, The effects of dark matter decay and annihilation on the high-redshift 21 cm background, Phys. Rev. D **74**, 103502 (2006).
[40] A. Natarajan and D. J. Schwarz, Dark matter annihilation and its effect on CMB and hydrogen 21 cm observations, Phys. Rev. D **80**, 043529 (2009).
[41] C. Garcia-Cely, A. Ibarra, and E. Molinaro, Cosmological and astrophysical signatures of dark matter annihilations into pseudo-Goldstone bosons, J. Cosmol. Astropart. Phys. 02 (2014) 032.
[42] Z. Chacko, Y. Cui, S. Hong, and T. Okui, A hidden dark matter sector, dark radiation, and the CMB, arXiv:1505.04192.
[43] S. Nussinov, Early inflation induced gravity waves can restrict astroparticle physics, arXiv:1408.1157.